Low-Temperature Rotational Relaxation of N_2 Studied with Resonance-Enhanced Multiphoton Ionization

F. J. Aoiz,[†] T. Díez-Rojo,[†,‡] V. J. Herrero,[*,‡] B. Martínez-Haya,[*,†] M. Menéndez,[†] P. Quintana,[†] L. Ramonat,[†,§] I. Tanarro,[‡] and E. Verdasco[†]

Departamento de Química Física, Facultad de Química, Universidad Complutense, E-28040 Madrid, Spain, and Instituto de Estructura de la Materia (CSIC), Serrano 113, E-28006 Madrid, Spain

Received: September 24, 1998; In Final Form: December 2, 1998

The rotational relaxation of molecular nitrogen has been investigated down to temperatures of about 5 K with a combination of resonance-enhanced multiphoton ionization and supersonic beam time-of-flight techniques. The average rotational relaxation cross section obtained shows a maximum value of 50−60 Å^2 at 20−30 K. For lower temperatures this cross section decreases and reaches a value smaller than 30 Å^2 at $T \approx 5$ K. For temperatures above 30 K, the cross section decreases slowly as the temperature grows and converges approximately to the determinations from other non-jet techniques and theoretical estimates available for $T > 80$ K. The results are compared to previous measurements from other groups using different methods, and general good agreement is found. However, we observe a significant discrepancy with some of the data from electron-beam-induced fluorescence that yield much larger cross sections for temperatures lower than 30 K.

1. Introduction

The rotational relaxation of molecular nitrogen has been studied over a wide temperature range with different experimental techniques including shock waves, thermal transpiration, ultrasonic methods, broadening coefficients of spectral lines, and various kinds of spectroscopic measurements performed on free jets (see, for instance, refs 1−9). Experimental data below ≈80 K have been derived exclusively from free jets and molecular beam experiments.[7,9−12] Theoretical treatments of varying complexity combining the gas dynamics of the supersonic flow with the kinetics of molecular energy transfer have been developed for the study of free jets,[8,13−19] but the lack of a precise knowledge of the flow field and of reliable data on the state-to-state energy transfer kinetics has precluded a rigorous comparison of theory and experiment. Ultimate progress in the field will certainly require more detailed calculations and thorough measurements of the local jet parameters with good spatial resolution.[20,21]

Theoretical values of the cross sections for N_2 rotationally inelastic collisions based on a direct solution of the three-dimensional (3D) equations of motion with a realistic intermolecular potential have been obtained using the method of quasiclassical trajectories (QCT),[22−25] but are restricted to date to temperatures above 100 K. For lower temperatures, theoretical estimates have been worked out with semiempirical models developed mostly from higher-temperature data (see refs 26−29 and references therein). Given the existing difficulties for the application of rigorous theoretical treatments, one must resort in general to very simple models involving drastic approximations in order to derive relaxation data from the measurements. In most cases the average rotational energy, characterized by a local rotational temperature, T_r, is assumed to be coupled to the translational temperature of the jet through a linear relaxation equation, and the actual degree of coupling between rotation and translation is described by an effective relaxation cross section, σ_r, or by another suitable parameter (relaxation time, τ_r, rotational collision number, z_r) related to σ_r.

Most experimental studies of N_2 rotational relaxation in supersonic free jets are based on the measurement of rotational temperatures using either Raman techniques or the electron-beam-induced fluorescence (EIF) method. Electron-beam-induced fluorescence has a high sensitivity and EIF measurements have been reported both along the axis of nitrogen free jets[5,7,30−32] and in the molecular beams extracted from them, at the end of the expansion.[10,11] However, the derivation of ground-state rotational populations from the EIF data is not trivial and can often be controversial (see, for instance, the discussion in refs 8 and 33 and in the references therein). In fact, the cross sections derived with the EIF method by different authors exhibit occasionally noteworthy discrepancies. For the ≈10−50 K temperature range, the reported σ_r values[5,17] can decrease from 200 to 40 Å^2 or have an average effective value of ≈14 Å^2,[10,11] depending mainly on the criteria followed for the data analysis.

Raman techniques provide a very direct sampling of the rovibrational state populations in the ground electronic state, but because of their comparatively low sensitivity, they cannot be easily applied to the measurement of rotational temperatures at the end of the expansion or in very low-density free jets, which are precisely the conditions for which the breakdown of equilibrium between translation and rotation is more clear. Although, in principle, the derivation of T_r from Raman measurements is nearly straightforward, significant discrepancies in the reported relaxation data can also be found in the literature. The σ_r inferred by the rotational collision numbers reported in the coherent antistokes Raman spectroscopy (CARS) experiment of ref 12 decrease from 200 to 80 Å^2 in the temperature interval 15−40 K, whereas those from the Stimulated Raman Spectros-

* Corresponding authors.
† Universidad Complutense.
‡ CSIC.
§ Present address: Hokkaido National Industrial Research Institute, 2-17-2-1, Tsukisamu-Higashi, Toyohira-ku, Sapporo 060, Japan.

10.1021/jp983850y CCC: $18.00
Published on Web 02/03/1999

copy (SRS) measurements of ref 9 vary from 50 to 30 Å^2 over the same temperature range.

In an attempt to clarify the discrepancies on the low-temperature rotational relaxation of N_2, we have used a different spectroscopic technique, namely resonance-enhanced multiphoton ionization (REMPI), for the measurement of rotational temperatures. This method was applied by Mazely and Smith[34] for the measurement of rotational temperatures along the axis of a free jet of nitrogen and has been applied more recently[35] to studies of relaxation in binary mixtures. Taking advantage of the high sensitivity of this technique, we have used it for the determination of the terminal rotational temperatures in the molecular beams skimmed from a large set of nitrogen free jets. In addition to the T_r measurements, terminal flow velocities and translational temperatures have been determined from time-of-flight (TOF) measurements. In this way, the end of the expansion and the breakdown of equilibrium between translation and rotation are sampled over a wide range of conditions. The validity of simple jet models is analyzed and the rotational relaxation cross sections obtained are discussed and compared to previous works.

The most relevant aspects of the experimental setup used in the present investigation are described in Section 2. The experimental results and their analysis are presented and discussed in detail in Section 3 and summarized in Section 4, where final conclusions are drawn.

2. Experimental Section

Free jets of pure nitrogen were formed by expanding the gas from a commercial solenoid-driven pulsed valve. The source pressures, p_0, ranged from ≈10 to 2500 mbar and the pulsed valve was kept at room temperature (T_o = 296 K) through all the measurements. The aperture time gate and voltage of the solenoid valve were set to generate nearly square gas pulses of 1 ms duration that were monitored with a fast ionization gauge. The TOF and REMPI measurements were performed on the central part of the gas pulses (quasi-steady-state), and special care was paid to the determination of the effective nozzle diameter, d_{eff}, from measurements of the gas flow to the expansion chamber.[36] The d_{eff} values were found to be ≈0.4 mm (±10%) as compared to the nominal diameter of 0.5 mm. The gas pulses were expanded into a 50 L chamber pumped by a 2000 L s^{-1} oil diffusion pump and the axial part of the expanding gas was collimated with a skimmer; the resulting molecular beams were then introduced into the REMPI or TOF analysis systems.

The setup for the REMPI measurements is shown schematically in Figure 1. The skimmer used for the connection between the expansion and the REMPI detection chamber is a commercial one of aerodynamic type (Beam Dynamics) with an approximate hyperbolic profile and a very thin wall (≈100 μm at the tip) having a 0.5-mm inner diameter. For the conditions of the present experiment, with mostly not-too-strong expansions and relatively large nozzle−skimmer distances, no significant skimmer interference is expected. Nevertheless, REMPI spectra for the largest values of $p_0 d_{eff}$ were also recorded for various nozzle skimmer distances in the 3.5−5.5 cm range, and no appreciable differences were observed. The source−skimmer distance was finally chosen within 4.0−5.5 cm at each working pressure in order to optimize the beam intensity in the detection chamber versus the effusive flow of background gas from the expansion chamber through the skimmer orifice. The detection chamber for the REMPI experiments was pumped by a 56 L s^{-1} turbomolecular pump. Typical pressures in the expansion and detection chambers during the experiments were 10^{-5}−10^{-4} and 10^{-6} mbar, respectively. Valve and laser were synchronized to a repetition rate of 10 Hz. The ionization UV radiation was focused with a 25-cm focal length lens in the beam axis, 21 cm downstream from the skimmer. The laser shot was delayed with respect to the pulsed valve in order to interact with the N_2 molecules 0.3 ms after the beginning of the 1-ms-long plateau of the gas pulse. No changes in the spectra were observed along the plateau except within 0.1 ms from the edges.

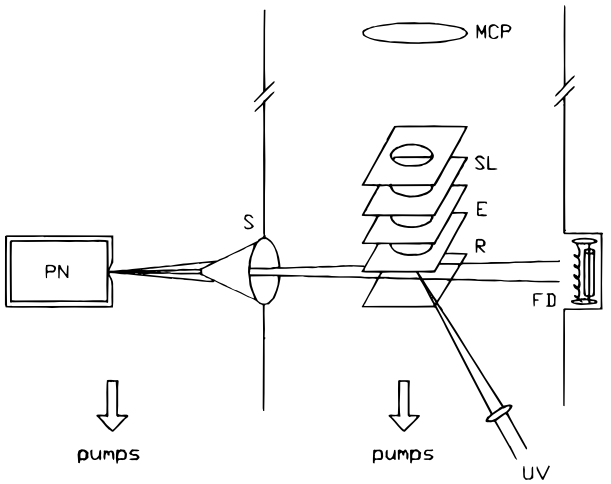

Figure 1. Schematic view of the experimental setup used for the REMPI measurements: PN, pulsed nozzle; S, skimmer; R, repeller; E, extractor; SL, steering plates; MCP, microchannel plate detector; FD, fast ionization detector; UV, ultraviolet laser beam.

N_2 is detected in a quantum state-specific manner by 2 + 2 REMPI via two-photon resonant excitation to the (1,0) vibrational band of the $a^1\Pi_g \leftarrow X^1\Sigma_g^+$ transition. The same laser pulse used to excite the initial two-photon transition also ionizes the excited molecule. The required tunable UV radiation at 283−285 nm was generated by frequency doubling of the output of a Nd:YAG-pumped dye laser (Continuum NY81-20/ND60). The dye laser was operated with a mixture of rhodamine 590 and 610 optimized to provide a flat output power between 560 and 578 nm. The UV laser pulses are linearly polarized and have time and frequency widths of 6 ns and 0.1 cm^{-1} (3 GHz), respectively. The power dependence of the REMPI signal was measured to be quadratic for pulse energies in the 1−3 mJ range. The experiments were run with 2 mJ/pulse and the measured ion intensities were corrected with the square of the laser energy at each wavelength, as given from the output of a fast photodiode recorded simultaneously to the ion signal. The laser focus (0.01 mm^3) intersected the axis of the supersonic molecular beam at the midpoint between the repeller and the extractor plates, which were at a distance of 10 mm from each other and were biased to V_0 = 1300 V and V_1 = 1050 V, respectively. The extractor plate is followed downstream toward the detector by three additional parallel plates with voltages dropping gradually to ground. The N_2^+ photoions are accelerated by the system of plates into a 21-cm-long field-free region toward a microchannel plate (Hamamatsu F2225-21S, diameter 42 mm). The time-dependent ion signal was recorded after amplification in a digital oscilloscope (Tektronix TDS524A) interfaced to a personal computer. The full width at half maximum (FWHM) of the temporal profile of the N_2^+ peak was 10 ns, and the oscilloscope was operated at 1 ns resolution.

The arrangement for the TOF measurements of the N_2 molecules has been described elsewhere,[9,36] and only the most relevant details will be given here. It consists of three interconnected vacuum chambers. The beam source is located in the

TABLE 1: Line Strengths, $S_{N'N''}$, for the Coherent Absorption of Two Linearly Polarized Photons Leading to the $a^1\Pi_g(v = 1, N') \leftarrow X^1\Sigma_g^+(v = 0, N'')$ Rotational Transitions of N_2

	O branch	P branch	Q branch	R branch	S branch
$S_{N'N''}$	$\frac{N''(N''-2)}{3(2N''-1)}$	$\frac{N''+1}{6}$	$\frac{2N''+1}{2(2N''+1)(2N''+3)}$	$\frac{N''}{6}$	$\frac{(N''+3)(N''+1)}{3(2N''+3)}$

first of these chambers, the second chamber houses a mechanical chopper and provides for differential pumping, and the third one houses the quadrupole mass spectrometer (QMS) used for detection and mass discrimination. The nozzle−skimmer distance was usually ≈4.5 cm, and the pulse frequency of the valve was made slow enough to keep the average background pressure in the 10^{-4}−10^{-5} mbar range in order to avoid attenuation of the beam. Two different skimmers were used in the measurements: the same aerodynamic skimmer used in the REMPI measurements for source pressures between ≈200 and 2500 mbar, and a conical one with a 1.8-mm diameter for the whole range of source pressures investigated (10−2500 mbar). This second skimmer was necessary in order to improve the signal-to-noise ratio in the TOF spectra of the beams coming from the weakest expansions. As indicated above, for the conditions of the present experiment no significant skimmer effects are expected and, in fact, in the range of p_0d_{eff} values studied with both skimmers, no appreciable differences were found in the velocity distributions derived from the measurements. In addition, TOF spectra for a fixed p_0d_{eff} were also recorded at different nozzle−skimmer distances between ≈3.5 and 5.5 cm, and again, no significant differences were detected in the time-of-arrival distributions even for the highest source pressures used. In the chopper chamber, beyond the skimmer, the pressure was lower than 5×10^{-6} mbar. The geometric gate function of the mechanical chopper used for the modulation of the gas pulses could be well approximated by a Gaussian curve with a FWHM of 31 and 22 μs for the larger and smaller skimmer, respectively. The molecules selected by the chopper were detected in the third chamber with the QMS under background pressure always in the 10^{-7} mbar range.

For the conditions of this experiment ($T_o = 296$ K, $d_{eff} \approx 0.04$ cm, $p_0d_{eff} \leq 100$ mbar cm), N_2 aggregation processes are expected to be negligible, and, in fact, no nitrogen dimers or higher aggregates were detectable with the QMS. The probability of dimer formation depends on the frequency of three-body collisions and should scale approximately with $p_0^2d_{eff}$. In ref 9, where the same source conditions and experimental setup were used for the TOF measurements, the onset of dimerization, estimated as the point where the QMS signal corresponding to the mass of the dimer ion is 0.5% of that of the monomer ion, was found at $p_0d_{eff} \approx 150$ mbar cm, which corresponds to a value of $p_0^2d_{eff}$ larger by a factor of 2 than that of the strongest expansions of the present work.

3. Results and Discussion

The terminal rotational temperatures of the different N_2 expansions studied were determined from the simulation of the molecular beam REMPI spectra. The intensity of each rotational line in the (2 + 2) REMPI spectrum is given by

$$I_{N'N''} = F \frac{S_{N'N''}}{2N''+1} P_{N''} \quad (1)$$

where $S_{N'N''}$ are the two-photon line strength factors for the $N' \leftarrow N''$ rotational transitions of the $a^1\Pi_g(v = 1) \leftarrow X^1\Sigma_g^+(v = 0)$ band as given in Table 1;[37] and F is a global (i.e., independent of N' and N'') normalization factor that accounts for the

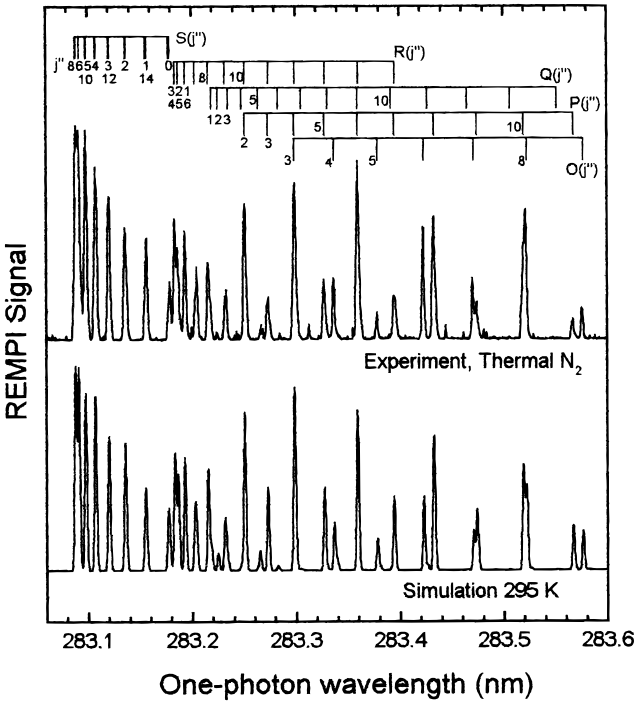

Figure 2. Experimental (top) and simulated (bottom) (2 + 2) REMPI spectra of N_2 at room temperature (see text for details).

vibrational and electronic parts of the two-photon absorption probability and for the absolute density of molecules in the ionization region. $P_{N''}$ represents the relative population of each rotational level N'' of the N_2 molecules. The $P_{N''}$ values were obtained from a linear least-square fit of the measured REMPI spectra. The $T_{r,\infty}$ values were then derived from the Boltzmann plots of the rotational populations. Within the error of the measurements, no significant deviations from Boltzmann distributions were obtained even for the highest N″ states. In particular, the same temperature correctly fits the population of the ortho (even N'') and para (odd N'') nitrogen species. These were treated as independent systems with spin−degeneracy weights of 2:1; that is, it is assumed that the room temperature ortho/para ratio in the source remains "frozen" during the supersonic expansion. Furthermore, it must be mentioned that the angular momentum of the N_2 molecules in the beam was assumed to be isotropically distributed in space, because no appreciable changes due to possible alignment effects were observed in REMPI measurements performed with different relative orientations of the laser polarization and the flow axis of the molecular beam.

The energies of the individual rotational levels E_r were calculated from a Dunham-type expansion with the coefficients given by Kompa and co-workers,[38] who concluded that both the ground state $X^1\Sigma_g^+(v = 0)$ and the excited state $a^1\Pi_g(v = 1)$ can be considered to be essentially free from perturbations due to predissociation and Λ-type doubling for rotational levels up to $N = 35$. Each rotational transition in the measured REMPI spectra was simulated with a peak of Lorentzian shape with a best-fit FWHM of 0.12 cm^{-1}. The whole spectrum, once calculated, was convoluted with a Gaussian function (FWHM

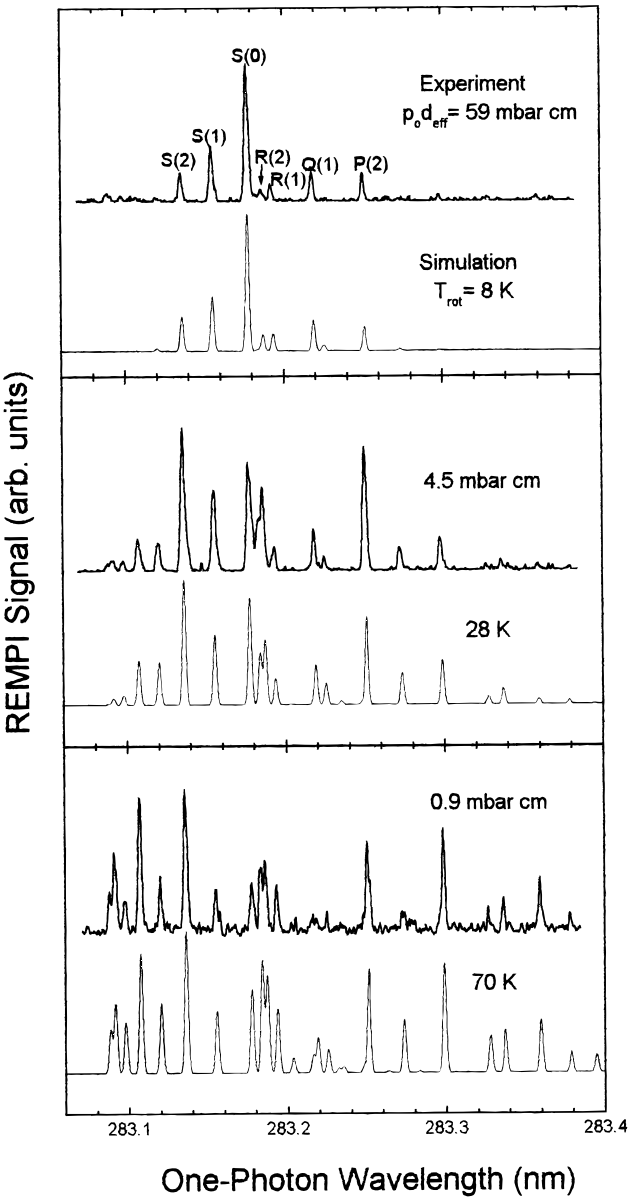

Figure 3. Three typical molecular beam REMPI spectra recorded for different expansion conditions. The simulated spectra and the best-fit rotational temperature $T_{r,\infty}$ used in the simulations are also shown for comparison.

0.10 cm^{-1}) to account for the instrumental contribution to the measured linewidth. The assignment of the observed rotational lines is given in detail in Figure 2, where the simulation of a room-temperature bulb spectrum is shown for reference.

Figure 3 shows three typical REMPI spectra recorded under different expanding conditions for the molecular beam. The simulated spectra, obtained in each case with the best-fit rotational temperature T_r, are also shown for comparison. As can be seen in the figures, the intensities of the peaks associated with the O, P, Q, R, and S rotational branches constitute a sensitive probe for the rotational temperature of the N_2 molecules in the supersonic molecular beam. The intense rotational cooling attained in the strongest expansions is apparent in this figure. At large source-stagnation pressures, $p_o > 1.5$ bar ($p_o d_{eff} > 60$ mbar cm), the measured spectra are dominated by the S(0) and S(1) transitions with a smaller contribution from the S(2), Q(1), and P(2) transitions (see upper panel of Figure 3), as corresponds to best-fit rotational temperatures of $T_r < 10$ K. A careful observation of the upper panel of Figure 3 reveals that in the spectra measured, for the most intense expansions a weak signal coming from background thermal molecules is also observed, which can be easily subtracted from the cold spectrum of the N_2 beam. With decreasing stagnation pressure the rotational temperature of the N_2 in the beam becomes progressively higher, as can be recognized in the REMPI spectra from the increasing relative intensity of the lines originating from excited rotational states. In the limit of a high Knudsen number, Kn_0 ($p_o d_{eff}$ = 0.4−0.6 mbar cm, $Kn_0 \approx 0.01$), the number of binary collisions during the expansion is extensively reduced, which leads to a poor rotational relaxation with best-fit temperatures as high as $T_r = 115 \pm 15$ K.

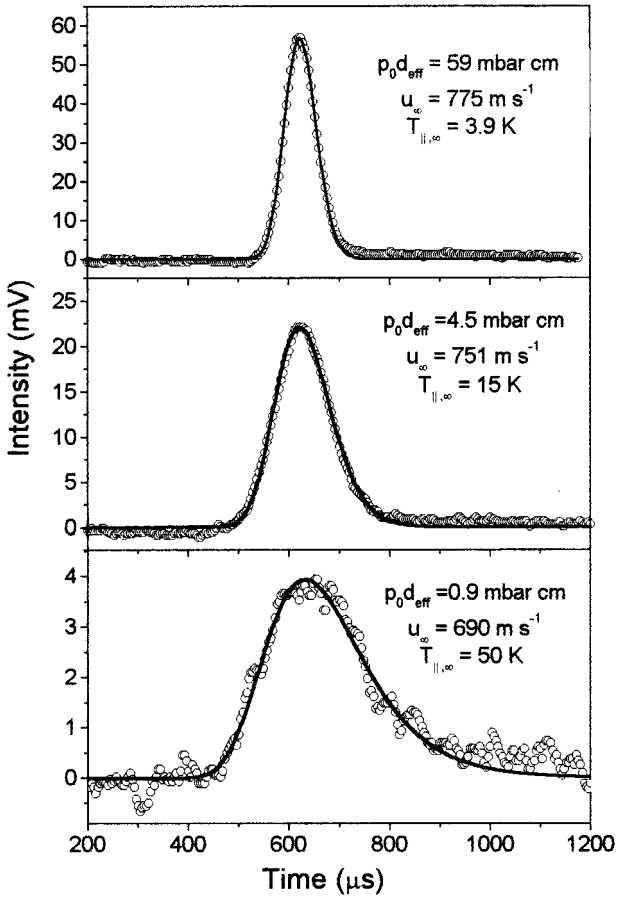

Figure 4. Time-of-arrival distributions measured in the molecular beams corresponding to three typical expansions: The points represent the experimental results and the solid line, the theoretical simulations. The best-fit terminal flow velocity, u_∞, and parallel translational temperature, $T_{||,\infty}$, are also indicated.

The final velocity distributions of the molecular beams were measured as in refs 9 and 36. The QMS detector sampled the velocity distribution parallel to the axial streamline of the expansion. We have made the usual assumption that this distribution is of the "drifting Maxwellian" type,[15] that is, a Maxwell distribution characterized by a temperature, $T_{||}$, traveling with the flow velocity, u. For a detector sensitive to the number density we have:[39] $f(v_{||}) \propto v_{||}^2 \exp[-(v_{||} - u)^2/\alpha_{||}^2]$, where $\alpha_{||} = (2kT_{||}/m)^{1/2}$, with k the Boltzmann constant and m the molecular mass. The terminal values of the flow velocity u_∞ and parallel temperature $T_{||,\infty}$ were obtained from the standard deconvolution of the TOF data.[40] Time-of-arrival distributions for three characteristic expansions are shown in Figure 4, together with their theoretical simulations.

The whole set of terminal flow velocities and translational and rotational temperatures measured in this work is shown in

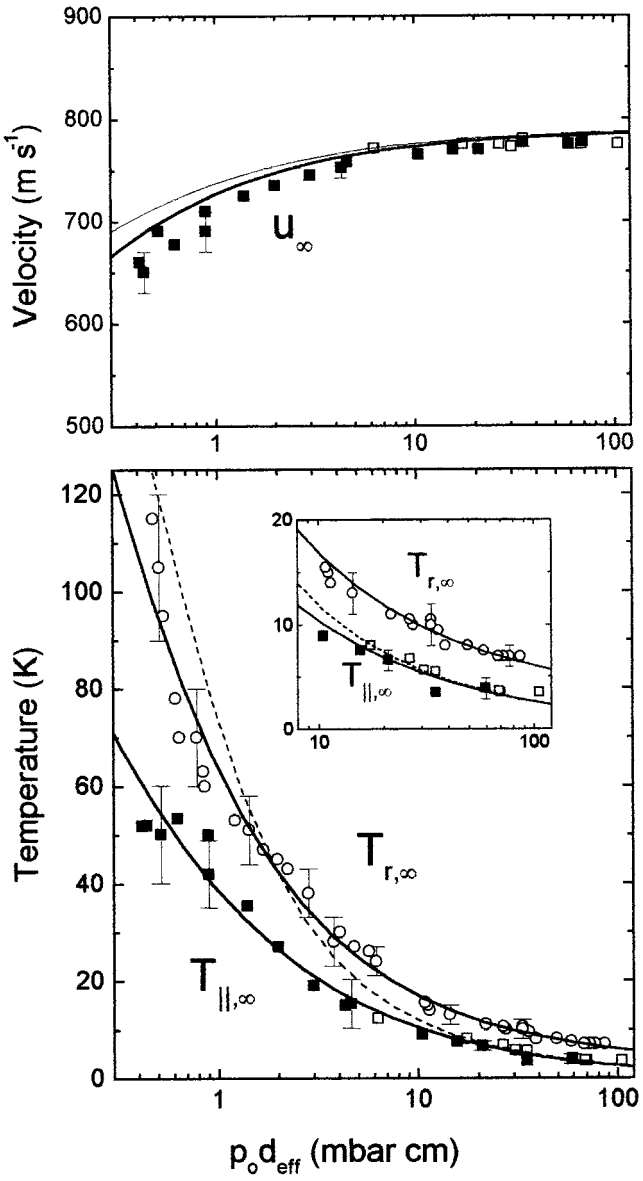

Figure 5. (Top) Terminal flow velocities, u_∞, as a function of $p_0 d_{eff}$. The points stand for experimental values. The thick solid line represents the terminal flow velocity obtained from energy conservation (eq 5), with the measured values of the terminal rotational and translational temperatures; the thin solid line represents the u_∞, corresponding to the $\gamma = 7/5$ isentropic behavior with the sudden freeze criterion used in the text. (Bottom) Circles and squares represent the measured terminal rotational and parallel translational temperatures, respectively, as a function of $p_0 d_{eff}$. Open and solid symbols refer to measurements performed with different types of skimmers (see text). Solid lines are the best-fit curves obtained with the present model. See text for details. The dashed curve is the prediction for $T_{r,\infty}$ derived from the relaxation cross sections of ref 7. The inset is an enlargement of the lowest-temperature region.

Figure 5. For the rationalization of these experimental data, we have made the same assumptions as in ref 9: (a) The supersonic expansion close to the axial streamline has an approximate spherical symmetry and is continuous, that is, describable in terms of local macroscopic variables, until a given distance ("quitting surface"). Beyond that point, collisions cease abruptly ("sudden freeze") and the flow becomes molecular. (b) The source energy is conserved along a streamline, the specific heat is constant, and the translational motion behaves in an approximately isentropic way. (c) In the continuous flow region the different molecular degrees of freedom may not be in equilibrium with each other, but thermal equilibrium is approximately maintained within each degree of freedom so that characteristic (Boltzmann) temperatures T_t, T_r, and T_v can be used for the description of the translational, rotational, and vibrational energetic modes, respectively. The N_2 vibrational degree of freedom does not participate in the expansion, given its very small room-temperature excitation and the high number of collisions required for its relaxation.[4] (d) Rotation is coupled to the translational thermal bath of the jet through

$$\frac{dT_r}{dt} = -\frac{1}{\tau_r}(T_r - T_t) \tag{2}$$

where τ_r represents the rotational relaxation time and T_t corresponds to the local translational temperature of the jet. The inverse of the rotational relaxation time can be viewed as the collision frequency for rotational relaxation and can be expressed in terms of an effective rotational relaxation cross section, σ_r, by means of $(\tau_r)^{-1} = 4n(kT_t/\pi m)^{1/2}\sigma_r$ where m is the molecular mass, k is the Boltzmann constant, and n is the jet local density.

Under the assumptions of the previous paragraph, the following balance equation, derived from the conservation of energy, holds along the jet centerline:[15]

$$T_0 = \frac{5}{7}T_t + \frac{2}{7}T_r + \frac{mu^2}{7k} \tag{3}$$

where it has been taken into account that the rotational contribution to the specific heat, C_r, is equal to k for a linear diatomic molecule. Toward the end of the expansion, when collisions cease, equilibrium is no longer maintained among the different components of the translational temperature. For expansions of approximate spherical symmetry, it is customary to consider a component parallel to streamlines, $T_{||}$, and two components perpendicular to streamlines, $T_\perp$. Within the sudden freeze model, $T_t = T_{||} = T_\perp$ along the continuous free jet until the quitting surface. As the expansion proceeds beyond this point, the perpendicular components of the translational temperature suffer a further geometrical cooling and tend to zero with increasing distance to the nozzle exit, but $T_{||}$, u, and T_r remain frozen. The u_∞ and $T_{||,\infty}$ determined from our TOF measurements hence correspond to the flow velocity and translational temperature at the quitting surface. These terminal flow velocities and translational temperatures are shown in the upper and lower panel of Figure 5, respectively, as a function of $p_0 d_{eff}$, which is a measure of the Knudsen number in the beam source. For a given $p_0 d_{eff}$ value, the measured terminal parallel temperature is taken as the criterion for the location of the quitting surface; that is, the expansion is assumed to proceed until the point where the isentropic temperature reaches $T_{||,\infty}$. The $T_{||,\infty}$ versus $p_0 d_{eff}$ data of the present work could be well fitted by modeling the terminal parallel speed ratio $S_{||,\infty} = (mu_\infty^2/2kT_{||,\infty})^{1/2}$, with the expression $S_{||,\infty} = 1.02(Kn_o)^{-0.31}$, in good agreement with the predictions of current models from the literature.[15,41]

For the derivation of $\sigma_r(T_t)$ from the present measurements, eq 2 is integrated numerically for each $p_0 d_{eff}$ along the jet axis until T_t reaches the value given by the best-fit curve to the measured $T_{||,\infty}$. At this point of the expansion, the calculated rotational temperature is compared to the measured $T_{r,\infty}$ and the rotational relaxation cross section is varied until a good fit to the experimental data is obtained. A functionality of the type

$$\sigma_r(T_t) = A\left(\frac{300}{T_t}\right)^{[1.3-(B/T_t)^{0.3}]} \tag{4}$$

was found to be flexible enough to account for the whole temperature interval relevant for our experiments. Similar expressions have been used in previous works.[7] The parameters giving a best fit to the data were $A = 13$ Å^2 and $B = 8$ K; the theoretical $T_{r,\infty}(p_0 d_{eff})$ obtained with these parameters is represented as a solid line in the lower panel of Figure 5, together with the measured temperatures. For the numerical integration of eq 2, the isentropic relations with $\gamma = 7/5$ were used in order to express the local Mach number, M, and derive the translational temperature, T_t, the jet number density, n, and the flow velocity, u, as a function of the distance to the nozzle exit.[15,43] This procedure does not take into account that the actual γ varies in the course of the expansion when the local rotational temperature lags behind the translational one. Although this approximation has proven to be adequate for small deviations of T_r from the isentropic behavior, it is not obvious that it should be appropriate here, given the wide range of expansion conditions sampled in the present work. In order to verify its validity, we tried also a correction suggested by Labowski et al.,[44] by adjusting the energy balance equation (eq 3) at each integration step. Terminal rotational temperatures obtained elsewhere with this correction were in good agreement with the results of a more rigorous calculation based on the method of characteristics.[15] In order to implement this correction, we used a $\gamma = 7/5$ equilibrium expansion, but decreased the external enthalpy by the amount corresponding to the "lagging" rotational energy $C_r \Delta T_r$. With the new source enthalpy thus obtained, the flow variables were rescaled before the next integration step. The terminal rotational temperatures obtained with a given $\sigma_r(T_t)$ were unaffected by this correction for $p_0 d_{eff}$ values larger than 0.8 mbar cm. For the lowest $p_0 d_{eff}$ investigated ($\approx$0.4 mbar cm), the corrected rotational temperatures were lower by about 3 K than those obtained by assuming a constant $\gamma = 7/5$; this difference is fully within the experimental uncertainty in the determination of $T_{r,\infty}$.

The energy balance at the quitting surface is readily obtained from eq 3 and from the considerations of the previous paragraphs as

$$T_0 = \frac{5}{7} T_{\parallel,\infty} + \frac{2}{7} T_{r,\infty} + \frac{m u_\infty^2}{7k} \qquad (5)$$

The energy balance equation at the end of the expansion has occasionally been used by other authors to obtain terminal rotational temperatures of N_2 with data from TOF measurements. However, this procedure is inaccurate, because most of the energy is carried by the flow velocity and a small experimental uncertainty in u_∞ leads to a large error in $T_{r,\infty}$.[9,10] In the present case, the terminal flow velocity and all the relevant temperatures have been determined experimentally, and one can use eq 5 in order to check the hypothesis of conservation of energy along the jet centerline. Since the introduction of a quitting surface is a gross oversimplification of the actual physical processes, it is not entirely clear where it must be placed. It should be stressed that, when checking the energy conservation, we have considered the translational temperature to be isotropic ($T_\parallel = T_\perp$) at the quitting surface, and thus we have also included the contribution of the perpendicular components at the end of the expansion, as reflected in eq 5. In previous works it has often been assumed that the energy balance is better satisfied by making $T_\perp \approx 0$ K, thus implying that the anisotropy in T_t begins before the actual freezing of $T_\parallel$.[13] Experimental measurements by Poulsen and Miller[10] seem to support this assumption, but as we shall see later, this is related to the higher rotational temperatures reported in ref 10, in comparison to the ones obtained in the present work.

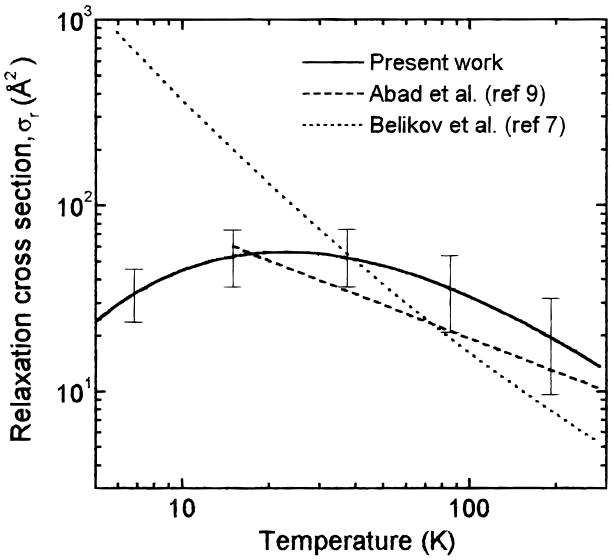

Figure 6. Cross section for the rotational relaxation of N_2 molecules as a function of temperature. Solid line with error bars, derived from the present REMPI experiments; dashed line, adapted from ref 9; dotted line, adapted from ref 7.

In the upper panel of Figure 5, the experimental u_∞ values are compared to those calculated with eq 5. The thick solid line represents the actual energy balance as obtained with the experimental temperatures (the best-fit curves for $T_{\parallel,\infty}$ and $T_{r,\infty}$ and $T_0 = 296$ K). The totally isentropic behavior ($T_{r,\infty} = T_{\parallel,\infty}$) for $\gamma = 7/5$ is also shown for reference in the figure with a thinner solid line. As can be seen, the measured values always lie slightly below the predictions of the energy balance equation. In particular, the experimental points become gradually lower than those from the energy balance curve with decreasing $p_0 d_{eff}$ in the $\approx$0.5−5.0 mbar cm range. This deviation cannot be entirely accounted for by the uncertainty in the determination of $T_{\parallel,\infty}$ or $T_{r,\infty}$. In this range, the source Knudsen number reaches comparatively high values ($Kn_o \approx 0.01$ for the mildest expansions considered). Under these circumstances, the assumption of ideal hydrodynamic flow underlying the isentropic model may not be justified and part of the source enthalpy might be lost because of heat conduction or viscous effects. In any case, the largest deviations observed are on the order of 5%, which means that, even for the lowest $p_0 d_{eff}$ values, more than 90% of the initial source energy is conserved along the jet centerline until the end of the expansion. For $p_0 d_{eff} > 10$ mbar cm, the deviations between the measurements and estimates of the energy balance equation are much smaller and the energy derived from the measured u_∞, $T_{\parallel,\infty}$ and $T_{r,\infty}$ account for 97−98% of that in the source. It should be noted that the assumption of $T_\perp \approx 0$ K, supported by the measurements of Poulsen and Miller,[10] would give even higher values of the terminal flow velocity and, consequently, a larger difference between the measured u_∞ and that from the energy balance.

The $\sigma_r(T_t)$ derived from the present REMPI measurements is represented in Figure 6 by a solid line with error bars. For temperatures lower than 300 K, the cross section grows with decreasing temperature and reaches a maximum of about 55 ± 20 Å^2 at $T_t = 20-30$ K. For lower temperatures, σ_r decreases down to $\approx$30 ± 10 Å^2 at $T_t = 5-10$ K. The sensitivity of the experiment decreases markedly for T_t higher than $\approx$80−100 K, but in this temperature region the present values agree approximately with those from quasiclassical trajectories[23] and

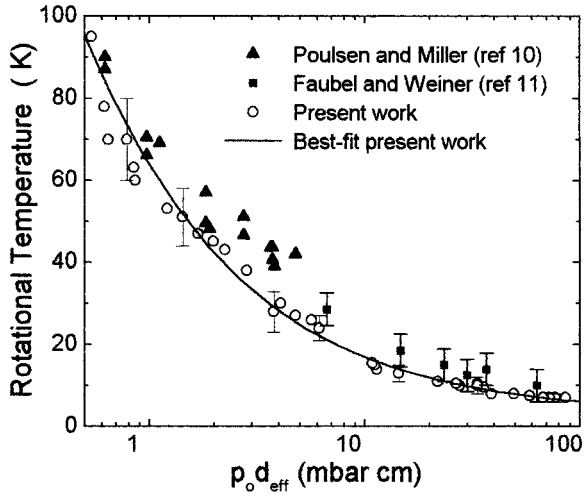

Figure 7. Terminal rotational temperatures as a function of p_0d_{eff}. Solid triangles, from ref 10. Solid squares, from ref 11. Open circles, present REMPI measurements. The solid line represents the best fit of present work. See text for details.

ultrasonic measurements.[3] In view of the relatively large uncertainties in σ_r and given its smooth evolution with temperature, it might be tempting at first sight to use an average constant relaxation cross section; however, this procedure does not give a good fit to the experimental data over the whole temperature range studied. Specifically, a decrease in σ_r below 20 K is needed in order to account for the final rotational temperatures of the strongest expansions. These results are compared in Figure 6 with the $\sigma_r(T_t)$ reported in two recent literature works. In both cases, a linear relaxation equation analogous to eq 2 and a translational temperature corresponding to that of the $\gamma = 7/5$ isentrope were assumed for the derivation of the rotational relaxation cross sections. The $\sigma_r(T)$ of Abad et al.,[9] which is based on the analysis of their free-jet SRS spectra and covers the temperature range 15−100 K, is consistent with the present results. However, the cross sections of Belikov et al.,[7] extending down to 6 K and based on EIF measurements performed also on free jets of N_2, are clearly at variance with the present ones in the temperature interval between 30 and 6 K, where the $\sigma_r(T_t)$ of ref 7 grows rapidly with decreasing T_t and reaches values of several hundred Å^2 below 15 K. The use of the $\sigma_r(T_t)$ of ref 7 within the model of the present work (integration of eq 2 until $T_t = T_{||,\infty}$) cannot reproduce the final rotational temperatures of our REMPI measurements as shown by the dashed line in Figure 5. In particular, the very large relaxation cross sections for the lowest T_t lead to $T_{r,\infty}$ values significantly smaller than those experimentally observed in our group at $p_0d_{\text{eff}} > 4$ mbar cm (see inset in Figure 5).

Terminal rotational temperatures measured with the EIF method in supersonic molecular beams of nitrogen from room-temperature sources have been reported by Poulsen and Miller[10] (for $p_0d_{\text{eff}} = 0.6-5.0$ mbar cm) and by Faubel and Weiner[11] (for $p_0d_{\text{eff}} = 6-66$ mbar cm). These results are compared in Figure 7 to the REMPI measurements of the present work. As indicated in the introduction, the deduction of ground-state rotational populations of N_2 from the electron-beam-induced fluorescence spectra is not straightforward. The method is based upon the promotion of ground-state nitrogen molecules $N_2(X^1\Sigma_g^+,v = 0,N)$ to the $N_2^+(B_g^+,^2\Sigma_u^+,v' = 0,N')$ ionic excited state by electron impact and subsequent study of the $N_2^+(B_g^+,^2\Sigma_u^+,v' = 0,N') \rightarrow N_2^+(X^2\Sigma_g^+,v'' = 0,N'')$ fluorescent emission. The main complications are related to the evaluation of the transition probabilities for the electron impact processes and to possible perturbations of the sample by the electron beam. In his pioneering work, Muntz[30] assumed dipole selection rules ($\Delta N = \pm 1$) for the primary excitation process. More recently, other groups[32,42,48,49] refined the model by introducing higher-order transitions ($\Delta N > 1$) associated with the presence of low-energy secondary electrons. In spite of these refinements, the interpretation of EIF data has remained controversial.[50−52] The need for a precise experimental determination of the electron impact transition probabilities and the convenience of verifying the electron beam results with data from optical spectroscopic methods have been stressed in a recent work.[33]

In the experiment of Poulsen and Miller, the "electric dipole" (ED) model of Munz[30] was used for the derivation of the rotational temperatures. In the work of Faubel and Weiner,[11] both the ED model and the "ejected electron interaction" (EEI) model of Coe et al.[32] were employed for the data analysis. Faubel and Wiener found that for a given set of points, the EEI model yields rotational temperatures lower by 30−40% than those of the ED model. For this experiment, the uncertainties in the rotational temperatures associated with the procedure for data analysis are shown as error bars in Figure 7. As can be seen, the EIF $T_{r,\infty}$ values from refs 10 and 11 are systematically higher than the present REMPI ones. In the two EIF experiments, an averaged (temperature-independent) rotational cross section, $\sigma_r \approx 14$ Å^2, was derived from the measured data by also using a sudden freeze model. This value for the cross section, when compared to our best-fit $\sigma_r(T_t)$ (Figure 6), reflects the discrepancies in $T_{r,\infty}$ shown in Figure 7 and is too low to account for our data, especially in the region of higher terminal temperatures (milder expansions) investigated by Poulsen and Miller. The disagreement is smaller with the measurements of Faubel and Weiner corresponding to lower terminal temperatures. Terminal translational temperatures were also provided in the mentioned works, and are coincident with ours within the mutual experimental uncertainty; they have not been represented in the figure for clarity of display.

Although in the present work no measurements have been performed in the free-jet region before the end of the expansion, the $\sigma_r(T_t)$ obtained from our data in conjunction with eq 2 can be used to simulate the free-jet results from previous literature works. In Figures 8 and 9, we show the results of such simulations. The data represented in Figure 8 correspond to optical spectroscopic methods, and those of Figure 9 correspond to EIF measurements. The calculated T_r, represented by solid curves, have been drawn until the position of the quitting surface, except in the lower panel of Figure 8, where the measured data stretch far beyond this point and the curve has been prolonged with a line corresponding to $T_{r,\infty}$.

The SRS measurements of Abad et al.[9] (Figure 8a) are satisfactorily reproduced with the rotational relaxation cross sections of the present work. It seems that in the lowest temperature region ($T_t < 10$ K) a smaller cross section could give a better fit, but the experimental uncertainty is too large to draw conclusions.

Figure 8b shows the simulation of the CARS measurements reported by Ilyukhin et al.[12] for two supersonic expansions without clustering. The simulation again gives a good global account for the data. For the stronger expansion, the experimental rotational temperatures do not deviate from the isentrope over the x/d_{eff} range studied, in accordance with the calculation. In this case the σ_r (T_t) of this work provides just a lower limit to that compatible with the measurements. For the milder expansion, the simulation yields values of T_r somewhat higher than the measured ones for temperatures lower than 20 K. It is

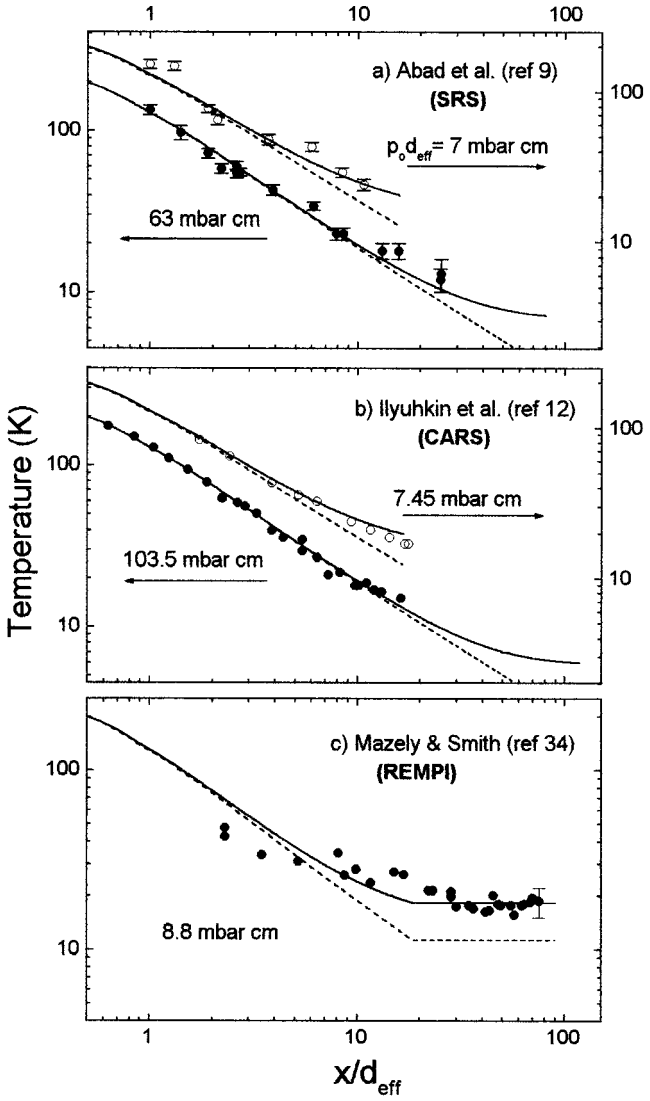

Figure 8. Simulations of rotational and translational temperatures in the free-jet expansions. In the three panels, the symbols are the experimental data obtained by optical spectroscopic methods and taken from the literature references indicated in the figures. The solid curves show the evolution of T_r calculated with eq 2 using the rotational cross sections obtained in the present work. The dashed line represents the evolution of the translational temperature, T_t which is assumed to be that of the $\gamma = 7/5$ isentrope.

worth noting that the rotational relaxation cross sections deducible from the rotational collision numbers, z_r, and gas kinetic cross sections, $\sigma_c(T_t)$, reported in ref 12 are larger than 100 Å^2 for temperatures below 30 K. Application of eq 2 with such large relaxation cross sections leads to T_r values lower than the experimentally measured ones for the milder expansion. The deviation of the curve calculated with the $\sigma_r(T_t)$ of ref 12 from the experimental points (not shown for clarity) is of similar magnitude but of opposite sign than that obtained with the present $\sigma_r(T_t)$. This fact reflects the comparatively low sensitivity of many jet measurements to the precise value of σ_r and stresses the usefulness of the present molecular beam experiments that sample terminal temperatures and evince the breakdown of equilibrium between translation and rotation in a more direct way.

Finally, Figure 8c displays the rotational temperatures for a relatively mild expansion of N_2 derived by Mazely and Smith[34] from REMPI measurements. In this case, the measured rotational temperatures sample the whole transition region from the free jet to the molecular flow. The location of the quitting surface is easily recognized as the point where the model T_r and T_t become frozen. Although the continuous free-jet data exhibit a certain dispersion, most of the points in the relevant asymptotic region are quite well reproduced with the present relaxation cross sections.

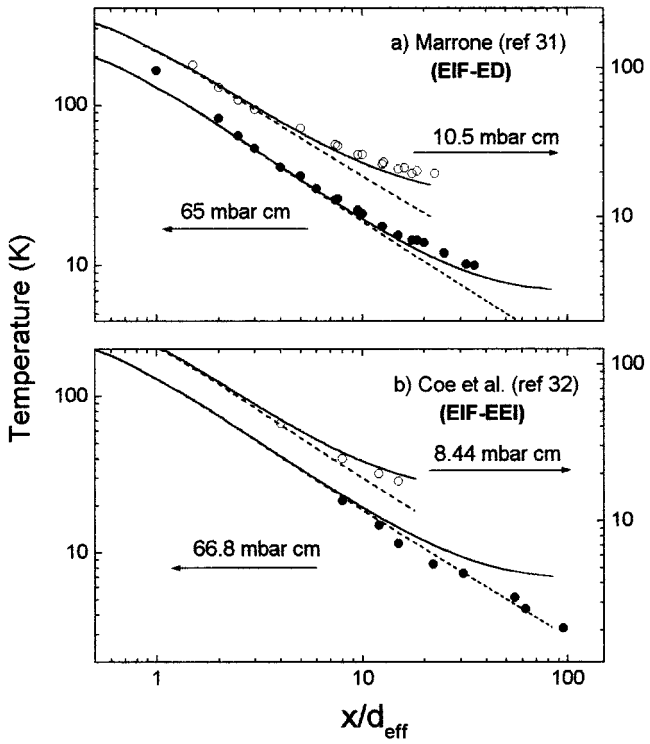

Figure 9. Same as Figure 8 but for EIF measurements.

Further measurements of the rotational temperature in free jets of nitrogen from room temperature sources from various Raman techniques[53−55] are also available in the literature (not shown in Figure 8). All these data are in good agreement with the temperatures predicted from the $\sigma_r(T_t)$ of this work.

Figure 9 shows the simulation of the results of two EIF experiments from different groups. In each case, a weak and a strong expansion with comparable $p_0 d_{eff}$ have been selected among the larger set studied by both groups. In the upper panel, the rotational temperatures obtained by Marrone[31] with the ED model are displayed. As can be seen, the overall trend, including the points of deviation of the rotational temperatures from the $\gamma = 7/5$ isentrope, is well reproduced by the calculated curves, but the experimental rotational temperatures are somewhat larger than those predicted with the present cross sections. In contrast to these results, the measurements of Coe et al.[32] (lower panel of Figure 9), who used the EEI model for the analysis of the fluorescence data, lead to rotational temperatures smaller than those predicted with our relaxation cross sections. Much higher cross sections than those obtained in this work would be necessary in order to account for the lowest temperature measurements. However, it is worth noting that, as shown by the authors, the same experimental data lead to higher temperatures and to a worse agreement with the assumption of a Boltzmann distribution for the rotational levels of the N_2 molecules in the jet, when the ED model is used for the analysis of the fluorescence spectra. Measurements of rotational temperatures in free jets of nitrogen by the EIF method have also been reported by other groups. A critical discussion of these results and of the conflicting interpretation of the data can be found in refs 8 and 33 and in the references cited therein.

The use of a rotational temperature in studies of rotational relaxation in free jets has sometimes been questioned because of the possibility of different relaxation kinetics for the individual rotational states.[35] Furthermore, for the very strong cooling attained in some of the jet experiments, the mere concept of a temperature for the characterization of the distribution of the few remaining rotational states may be dubious. In this respect, it should be noted that a possible departure from Boltzmann equilibrium would not invalidate the estimates of the average relaxation cross section obtained with eq 2, because T_r can be considered as a convenient shorthand for the average rotational energy. The actual occurrence of non-Boltzmann distributions of rotational levels in free jets of N_2 has been much debated. In many of the EIF experiments an overpopulation of the higher rotational levels is found, whereas in all of the experiments based on optical spectroscopic methods mentioned above, approximate Boltzmann distributions are reported within the experimental uncertainty. In the present work no significant deviation from Boltzmann type populations was observed even for the coldest supersonic beams investigated, for which the relative population of rotational states is well reproduced with temperatures as low as $T_r \approx 7$ K (see Figure 3). In any case, there seems to be a general agreement about the fact that for the lower levels, where most of the rotational energy is concentrated, the assumption of a Boltzmann distribution is justified.

The considerations of the previous paragraphs indicate that a good overall agreement exists between the results of this work and most of the measurements from other groups based on optical spectroscopic methods, but discrepancies are found with some of the EIF results, both in the higher[10] and lower[7,32] end of the temperature range investigated. The most significant discrepancy between the results of this work and others from the literature concerns the magnitude of the rotational relaxation cross sections for temperatures lower than 20 K. Whereas our results indicate that $\sigma_r(T_t)$ has an average value of $\approx$30 Å^2 in the 5−25 K temperature interval, the relaxation cross sections reported by Belikov et al.[7] or those implied by the T_r measured by Coe et al.[32] are much larger (by several hundred Å^2) and certainly incompatible with our data.

In the absence of accurate dynamical calculations for the low-temperature interval relevant to the observed discrepancy, we will give a simple and intuitive argument in qualitative support of our results. A rough estimate of the likelihood of rotational energy transfer by collisions is provided by the adiabaticity or Massey parameter,[4,56] $\xi = t_{coll}/t_{rot}$, where t_{coll} represents the collision time and t_{rot} the rotational period. The collision time is usually defined as $a/\langle v \rangle$, where a is the range of the intermolecular potential and the average collision velocity is given by $\langle v \rangle = (8kT_t/\pi m)^{1/2}$. The probability of rotational energy transfer decreases with increasing ξ, and the region of $\xi > 1$ (collision slower than rotation) is generally taken as the adiabatic regime of inefficient energy transfer. In Figure 10 we have represented the evolution of ξ with temperature for our system, together with our best-fit $\sigma_r(T_t)$. For the calculation of t_{rot} at a given temperature, we have taken average rotational period of the rotational levels, N, that can relax (i.e., those with $N \geq 2$), and for the calculation of t_{coll} we have assumed that $a \approx 3.8$ Å is the length parameter of a N_2-N_2 Lennard-Jones potential. As can be seen, ξ increases abruptly at low temperature, $T < 30$ K, toward the adiabatic regime, precisely where our observations yield a marked decrease of the rotational relaxation cross section. Hence, these qualitative considerations are congruent with our data and render very unlikely a large increase of the rotational relaxation probability in the 5−30 K temperature range, as proposed in previous works.

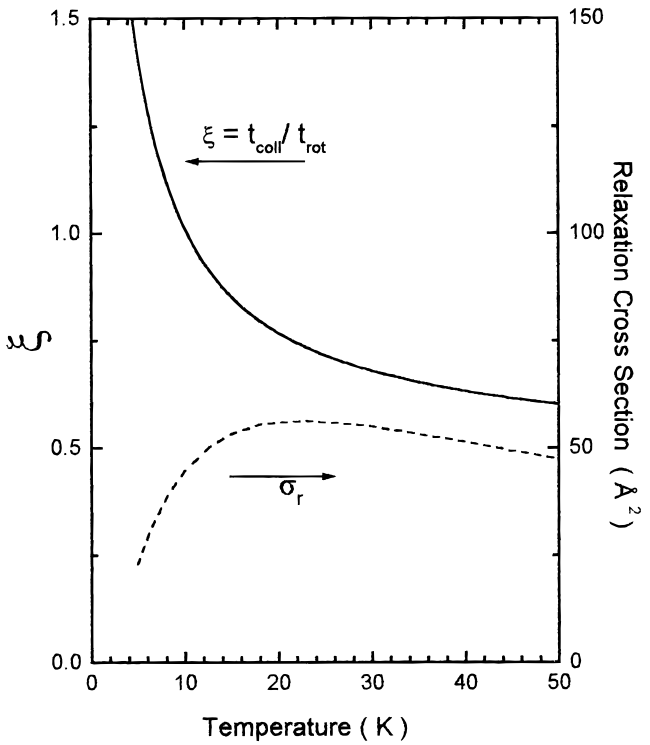

Figure 10. Evolution of the Massey parameter, ξ, with temperature together with the best-fit $\sigma_r(T_t)$ from the present work.

4. Summary and Conclusions

The technique of resonance-enhanced multiphoton ionization has been applied to the determination of terminal rotational temperatures in supersonic molecular beams extracted from free jets of nitrogen. These data, together with measurements of terminal flow velocities and translational temperatures obtained from TOF measurements, have been used for the estimate of the cross section for rotational energy relaxation at low temperature ($T \approx 5-100$ K).

The present data suggest that the isentropic hypothesis used in most free-jet models is, in general, well justified. For hydrodynamic expansions of N_2 from room-temperature sources, the condition of conservation of energy along the jet centerline, underlying isentropic behavior is fulfilled within 97−98% for values of the source Knudsen number smaller than 0.001 and, even for $Kn_0 \approx 0.01$, more than 90% of the source energy is conserved at the end of the expansion.

From our terminal rotational temperatures, the average relaxation cross section has been estimated over a wide temperature range extending down to approximately 5 K. The cross sections for rotational relaxation found in this work have a maximum value of approximately 50−60 Å^2 at 20−30 K. For lower temperatures this cross section decreases and reaches a value smaller than 30 Å^2 at $T \approx 5$ K. At temperatures higher than 30 K, the cross section decreases slowly with growing temperature and converges approximately to the determinations from other non-jet techniques and theoretical estimates for $T \approx$ 80−100 K.

The literature values of free-jet rotational temperatures measured with different optical spectroscopic methods are, in general, well reproduced with the relaxation cross section derived from our experimental data. The results from electron-beam-induced fluorescence experiments are more dependent on

the data reduction scheme, and, for temperatures lower than 30 K, some of these experiments yield very large cross sections clearly at variance with the findings of the present work. Classical arguments based on the value of the Massey parameter support the present data and show that for the low temperatures investigated, collisions tend to enter the adiabatic regime, where the probability of energy transfer between rotation and translation should decrease markedly. Nevertheless, further experiments and theoretical calculations are needed in order to assess the likelihood of rotational relaxation of nitrogen at very low temperatures.

Acknowledgment. B.M.-H. acknowledges support from the program "Incorporación a España de Doctores y Tecnólogos" of the Spanish Ministerio de Educación y Ciencia (MEC) and from the program "Ayuda a la Investigación" of the Fundación Caja de Madrid. T.D.-R. and P.Q. acknowledge grants from the FPI program of the MEC. This work was financed by the MEC of Spain under *DGICYT* Project PB95/0918-C03. We also acknowledge the facilities provided by the "CAI de Espectroscopía" of the Universidad Complutense de Madrid, where the REMPI measurements were carried out.

References and Notes

(1) Robben, F.; Talbot, L. *Phys. Fluids* **1966**, *9*, 633.
(2) Butherus, T. F.; Storvik, T. S. *J. Chem. Phys.* **1974**, *60*, 321.
(3) Prangsma G. J.; Alberga, A. H.; Beenakker, J. J. M. *Physica* **1973**, *64*, 278.
(4) Lambert, J. D. *Vibrational and Rotational Relaxation in Gases;* Oxford University Press: Oxford, 1977.
(5) Belikov, A. E.; Sukhinin, G. I.; Sharafutdinov, R. G. *Rarefied Gas Dynamics, 16th Symposium*; Muntz, E. P., Weaver D. P., Campbell, D. H., Eds.; Progress in Astronautics and Aeronautics; AIAA Inc.: Washington, 1989; Vol. 117, p 50.
(6) Temkin, S.; Thuet, J. M.; Bonamy, J.; Robert, D. *Chem. Phys.* **1991**, *158*, 89.
(7) Belikov, A. E.; Sharafutdinov, R. G.; Strekalov, M. L. *Chem. Phys. Lett.* **1994**, *231*, 444.
(8) Campargue, R.; Gaveau, M. A.; Lebéhot, A. *Rarefied Gas Dynamics, 14th Symposium*; Oguchi, H., Ed.; University of Tokyo Press: Tokyo, 1984. Vol. II, p 551.
(9) Abad, L.; Bermejo, D.; Herrero, V. J.; Santos, J.; Tanarro, I. *J. Phys. Chem. A* **1997**, *101*, 9276.
(10) Poulsen, P.; Miller, D. R. *Rarefied Gas Dynamics, 10th Int. Symposium*; Potter, J. L., Ed.; Progress in Astronautics and Aeronautics; AIAA: New York, 1977; Vol. 51, p 899.
(11) Faubel, M.; Weiner, E. R. *J. Chem. Phys.* **1981**, *75*, 641.
(12) Ilyukhin, A. A.; Pykhov, R. L.; Smirnov, V. V.; Marowski., G. *Appl. Phys. B.* **1990**, *51*, 1992.
(13) Hamel, B. B.; Willis, D. R. *Phys. Fluids* **1966**, *9*, 829.
(14) Rabitz, H.; Lam, S. H. *J. Chem. Phys.* **1975**, *63*, 3532.
(15) Miller, D. R. *Atomic and Molecular Beam Methods*; Scoles, G., Ed.; Oxford University Press: New York, 1988; Vol. 1.
(16) Klots, C. E. *J. Chem. Phys.* **1980**, *72*, 192.
(17) Belikov, A. E.; Burshtein, A. I.; Doglgushev, S. V.; Storozhev, A. V.; Strekalov, M. L.; Shukhinin, G. I.; Sharafutdinov, R. G. *Chem. Phys.* **1989**, *139*, 239.
(18) Randeniya, L. K.; Smith, M. A. *J. Chem. Phys.* **1990**, *93*, 661.
(19) Cameron, B. R.; Harland, P. W. *J. Chem. Soc., Faraday Trans.* **1993**, *89*, 1903.
(20) Tejeda, G.; Maté, B.; Fernández Sánchez, J. M.; Montero, S. *Phys. Rev. Lett.* **1996**, *76*, 34.
(21) Maté, B.; Tejeda, G.; Montero, S. *J. Chem. Phys.* **1998**, *108*, 2676.
(22) Turfa, A. F.; Knaap, H. F. P.; Thijsse, B. J.; Beenhakker, J. J. M. *Physica A* **1982**, *112*, 18.
(23) Nyeland, C.; Poulsen, L. L.; Billing, G. D. *J. Phys. Chem.* **1984**, *88*, 1216.
(24) Nyeland, C.; Billing, G. D. *J. Phys. Chem.* **1988**, *92*, 1752.
(25) Billing, G. D.; Wang, L. *J. Phys. Chem.* **1992**, *96*, 2672.
(26) Steinfeld, J. I.; Ruttenberg, P.; Millot, G.; Fanjoux, G.; Lavorel, B. *J. Phys. Chem.* **1991**, *95*, 9638.
(27) Cameron, B. R.; Harland, P. W. *J. Chem. Soc., Faraday Trans.* **1993**, *89*, 3517.
(28) Strekalov, M. L. *Mol. Phys.* **1995**, *86*, 39.
(29) Sharafutdinov, R. G.; Belikov, A. E.; Strekalov, M. L.; Storozhev, A. V. *Chem. Phys.* **1996**, *207*, 193.
(30) Muntz, E. P. *Phys. Fluids* **1962**, *5*, 80.
(31) Marrone, P. V. *Phys. Fluids* **1967**, *10*, 521.
(32) Coe, D.; Robben, F.; Talbot, L.; Cattolica, R. *Phys. Fluids*; **1980**, *23*,715.
(33) Sukhinin, G. I.; Sharafutdinov, R. G.; Belikov, A. E.; Sedelnikov, A. I. *Chem. Phys.* **1994**, *189*, 603.
(34) Mazely, T. L.; Smith, M. A. *J. Phys. Chem.* **1990**, *94*, 6930.
(35) Belikov, A. E.; Aherm, M. M.; Smith, M. M. *Chem Phys.* **1998**, *234*, 195.
(36) Abad, L.; Bermejo, D.; Herrero, V. J.; Santos, J.; Tanarro, I. *Rev. Sci. Instrum.* **1995**, *66*, 3826.
(37) Bray, R. G.; Hochstrasser, R. M. *Mol. Phys.* **1976**, *31*, 1199.
(38) Trickl, T. ; Proch, D.; Kompa, K.L. *J. Mol. Spectrosc.* **1993**, *162*, 184.
(39) Haberland, H.; Buck, U.; Tolle, M. *Rev. Sci. Instrum.* **1985**, *56*, 1712.
(40) Auerbach, D. J. *Atomic and Molecular Beam Methods*; Scoles, G., Ed.; Oxford University Press: New York, 1988; Vol. 1.
(41) Beijerinck, H.; Verster, N. *Physica* **1981**, *111C*, 327.
(42) Belikov, A. E.; Zarvin, A. E.; Karelov, N. V.; Sukhinin, G. I.; Sharafutdinov, R. G. *Zh. Prikl. Tekhn. Fiz.* **1984**, *3*, 5.
(43) Quah, C. G. *Chem. Phys. Lett.* **1979**, *63*, 141.
(44) Labowsky, M.; Ryali, S. B.; Fenn, J. B.; Miller, D. R. *Rarefied Gas Dynamics, 12th Symposium*; Muntz, S. S, Ed.; Progress in Astronautics and Aeronautics; AIAA Inc.: New York, 1981; Vol. 74 (II), p 695.
(45) Miller, D. R.; Andres, R. P. *J. Chem. Phys.* **1967**, *46*, 3418.
(46) Gallagher, R. J.; Fenn, J. B. *J. Chem. Phys.* **1974**, *60*, 3487.
(47) Yamazaki, S.; Taki, M.; Fujitani, Y. *J. Chem. Phys.* **1981**, *74*, 4476.
(48) Rebrov, A. K.; Sukhinin, G. I.; Sharafutdinov, R. G.; Lengrand, J. C. *Sov. Phys. Tech. Phys.* **1981**, *26*, 1062.
(49) DeKoven, B. M.; Levy, D. H.; Harris, H. H.; Zegarski, B. R.; Miller, T. A. *J. Chem. Phys.* **1981**, *74*, 5659.
(50) Hernandez, S. P.; Dagdigian, P. J.; Doering, J. P. *Chem. Phys. Lett.* **1982**, *91*, 409.
(51) Helvajian, H.; Dekoven, B. M.; Baronavski, A. P. *Chem. Phys.* **1984**, *90*, 175.
(52) Zetner, P. W.; Darrach, M.; Hammond, P.; Westerweld, W. B.; McConkey, R. L. *Chem. Phys.* **1988**, *124*, 453.
(53) Luijks, G.; Stolte, S.; Reuss, J. *Chem. Phys.* **1981**, *62*, 217.
(54) Valentini, J. J.; Esherick, P.; Owyoung, A. *Chem. Phys. Lett.* **1980**, *75*, 1980.
(55) Huber-Wälchli, P.; Nibler, J. W. *J. Chem. Phys.* **1982**, *76*, 273.
(56) Levine, R. D.; Berstein, R. B. *Molecular Reaction Dynamics and Chemical Reactivity*; Oxford University Press: New York, 1987.